48 *Chem. Mater.* **2011,** *23,* 48–56
DOI:10.1021/cm102925z

CHEMISTRY OF MATERIALS
Article

Direct Hydrothermal Synthesis and Physical Properties of Rare-Earth and Yttrium Orthochromite Perovskites

Kripasindhu Sardar,[†] Martin R. Lees,[‡] Reza J. Kashtiban,[‡] Jeremy Sloan,[‡] and Richard I. Walton*[,†]

[†]*Department of Chemistry and* [‡]*Department of Physics, University of Warwick, Coventry CV4 7AL, U.K.*

Received October 11, 2010. Revised Manuscript Received November 19, 2010

We describe a systematic study of the hydrothermal synthesis of rare-earth orthochromites, $RCrO_3$ (R = La, Pr, Sm, Gd, Dy, Ho, Yb, and Lu) and $YCrO_3$. All nine of these materials can be prepared in a single step by hydrothermal treatment of an amorphous mixed-metal hydroxide at temperatures above 300 °C upon heating around 24 h, with no post-synthesis annealing needed. The as-made materials are highly crystalline powders with submicrometer particle size. In the case of $LaCrO_3$ the addition of solution additives to the hydrothermal synthesis allows some modification of crystallite form of the material, and in the presence of sodium dodecylsulfate nanocrystalline powders are produced. Profile refinement of powder X-ray diffraction (XRD) data show that each of the $RCrO_3$ materials adopts an orthorhombic distorted (*Pbmn*) perovskite structure. Detailed, magnetization studies as a function of temperature reveal the high quality of the specimens, with low temperature antiferromagnetic behavior seen by direct current (DC) magnetization, and T_N values that correlate with the structural distortion. A high temperature structural phase transition ($\sim$ 540 K to rhombohedral $R\bar{3}c$) seen by variable temperature XRD in the hydrothermally prepared $LaCrO_3$ is consistent with the reported behavior of the same composition prepared using conventional high temperature synthesis.

Introduction

The synthesis, structural, magnetic, and electrical properties of perovskite orthochromites containing rare-earth elements with general formula $RCr^{III}O_3$ (where R is a rare-earth element; La−Lu) have been well documented in the chemistry and physics literature over the last few decades.[1−5] The recent theoretical prediction of magnetoelectric coupling between the rare-earth and Cr^{3+} ions, along with the experimental observation of multiferroic properties in some of the rare-earth orthochromites has renewed interest in these materials.[6,7] The $RCrO_3$ materials are p-type semiconductors that have been reported to show electronic sensitivity toward humidity, methanol, ethanol, and gases such as H_2, CO, NO, N_2O, and so forth, a property that is useful for sensor applications.[4,8] Furthermore, $LaCrO_3$ and its doped variants (e.g., where La^{3+} is replaced with Ca^{2+} or Sr^{2+}) exhibit favorable sintering properties, high electrical conductivity and stability in reducing atmosphere, which make them promising candidates as interconnect materials in solid oxide fuel cells.[9] Finally, catalysis properties toward hydrocarbon oxidation have been investigated for some doped chromites.[10]

Traditional synthesis of bulk powders of ABO_3 perovskite oxides involves solid-state reaction of stoichiometric mixtures of the appropriate metal oxides at temperatures in excess of 1000 °C with multiple reheating and regrinding essential to overcome the barrier of diffusion in the solid state. Other synthesis methods reported in the literature for the case of $RCrO_3$ perovskites include self-propagating high temperature synthesis,[11] metathesis of metal chlorides,[12] decomposition of co-precipitated precursors,[13] citrate sol−gel route,[14] hydrazine method,[15] spray pyrolysis,[16] and polyol mediated synthesis.[17]

*To whom correspondence should be addressed. E-mail: r.i.walton@warwick.ac.uk.

(1) Bertaut, N. E. F.; Bassi, G.; Buisson, G.; Burlet, P.; Chappert, J.; Delapalme, A.; Mareschal, J.; Roult, G.; Aleonard, R.; Pauthenet, R.; Rebouillat, J. P. *J. Appl. Phys.* **1966**, *37*, 1038.
(2) Geller, S. *Acta Crystallogr.* **1957**, *10*, 243. Subbarao, G. V.; Wanklyn, B. M.; Rao, C. N. R. *J. Phys. Chem. Solids* **1971**, *32*, 345.
(3) Satoh, H.; Koseki, S.; Takagi, M.; Chung, W. Y.; Kamegashira, N. *J. Alloys Compd.* **1997**, *259*, 176. Shamir, N.; Shaked, H.; Shtrikman, S. *Phys. Rev. B* **1981**, *24*, 6642. Tripathi, A. K.; Lal, H. B. *Mater. Res. Bull.* **1980**, *15*, 233.
(4) Siemons, M.; Simon, U. *Sens. Actuators, B* **2007**, *126*, 181.
(5) Tsushima, K.; Aoyagi, K.; Sugano, S. *J. Appl. Phys.* **1970**, *41*, 1238.
(6) Sahu, J. R.; Serrao, C. R.; Ray, N.; Waghmare, U. V.; Rao, C. N. R. *J. Mater. Chem.* **2007**, *17*, 42.
(7) Serrao, C. R.; Kundu, A. K.; Krupanidhi, S. B.; Waghmare, U. V.; Rao, C. N. R. *Phys. Rev. B* **2005**, 72. Zvezdin, A. K.; Mukhin, A. A. *JETP Lett.* **2008**, *88*, 505.
(8) Russo, N.; Mescia, D.; Fino, D.; Saracco, G.; Specchia, V. *Ind. Eng. Chem. Res.* **2007**, *46*, 4226. Lakshmi, D.; Sundaram, R. *Sens. Transducers J.* **2008**, *97*, 74.
(9) Fergus, J. W. *Solid State Ionics* **2004**, *171*, 1. Tompsett, G. A.; Sammes, N. M. *J. Power Sources* **2004**, *130*, 1.
(10) Beckers, J.; Rothenberg, G. *ChemPhysChem* **2005**, *6*, 223.
(11) Kuznetsov, M. V.; Parkin, I. P. *Polyhedron* **1998**, *17*, 4443.
(12) Parkin, I. P.; Komarov, A. V.; Fang, Q. *Polyhedron* **1996**, *15*, 3117.
(13) Inagaki, M.; Yamamoto, O.; Hirohara, M. *J. Ceram. Soc. Jpn.* **1990**, *98*, 675.
(14) Devi, P. S. *J. Mater. Chem.* **1993**, *3*, 373.
(15) Kikkawa, T.; Yoshinaka, M.; Hirota, K.; Yamaguchi, O. *J. Mater. Sci. Lett.* **1995**, *14*, 1071.
(16) Vernoux, P.; Djurado, E.; Guillodo, M. *J. Am. Ceram. Soc.* **2001**, *84*, 2289.
(17) Siemons, M.; Leifert, A.; Simon, U. *Adv. Funct. Mater.* **2007**, *17*, 2189.

Published on Web 12/13/2010

Although most of these routes do reduce the crystallization time of orthochromites by eliminating the extended period of heating associated with diffusion-controlled, solid−solid reactions (by virtue of intimate mixing of reagents in short times), usually a high temperature annealing step is still required to bring about crystallinity. For example in the polyol mediated synthesis route an annealing step at up to 900 °C is required to induce crystallinity and also to burn off organic complexing ligands.[17] This is in fact typical of many '*chimie douce*' methods.

One-step solution methods for metal oxides are required to introduce greater control over the crystal growth, which might permit novel crystal morphologies that allow optimization of physical properties, or means of fabrication of devices. In this respect, solvothermal synthesis methods are attractive and indeed have already been used for the single-step preparation of a number of important perovskite families,[18] including ferroelectrics such as $BaTiO_3$,[19] $PbZr_{1-x}Ti_xO_3$,[20] and $Na_{1-x}K_xNbO_3$[21] and the mixed-valent manganites $Ln_{1-x}A_xMnO_3$ (Ln = La, Pr, Nd, etc., and A = Ca, Sr, Ba).[22] Here, the crystalline solids are formed directly from solution at temperatures as low as 80 °C although typically 150−200 °C would be required. The hydrothermal synthesis of chromite perovskites, in contrast, has been the focus of fewer studies. Early work by Yoshimura, Song, and co-workers suggested that for $LaCrO_3$ hydrothermal synthesis was only possible if temperatures above 400 °C were used.[23] The temperatures of reaction were revised in later work by Rivas-Vazquez et al. who were able to prepare Ca-doped $LaCrO_3$ only above 350 °C using hydrothermal conditions,[24] and Zheng et al. found that the temperature of synthesis could be lowered to 260 °C if high KOH concentrations were used in the synthesis of $LaCrO_3$.[25] In contrast, Ovenstone et al. found that Ca- and Sr-doped $LaCrO_3$ was not formed directly from solution when acetate precursors were used with ammonia as a base, and subsequent annealing in excess of 1000 °C was needed to produce highly crystalline chromite perovskites.[26]

In light of the current potential applications of the orthochromites, simple synthetic approaches to the materials are clearly desirable. From the above discussion it can be seen that the only work on hydrothermal synthesis of orthochromites so far has focused on $LaCrO_3$ and its doped analogues. In this paper we describe a systematic investigation of the use of hydrothermal methods as a means of the single-step preparation of a range of rare-earth orthochromites and $YCrO_3$, and a comprehensive study of their properties, including detailed magnetic characterization that confirms the high quality polycrystalline materials that can be prepared by this route.

Experimental Section

Synthesis. The hydrothermal synthesis of $RCrO_3$ materials was undertaken by first preparing an amorphous mixed-metal hydroxide material from appropriate hydrated salts using rare-earth chlorides or nitrates (or YCl_3) and chromium(III) nitrate (See Supporting Information for full details). In a typical synthesis, to a clear aqueous solution containing an equimolar ratio of Cr (III) nitrate and respective rare-earth (III) salt (or yttrium(III) chloride), 10−12 M KOH solution was added in excess to ensure the complete formation of metal hydroxides. The suspension containing hydroxides was stirred for 10 min, and then filtered using suction, followed by washing with copious amounts of deionized water. The precipitate thus obtained was dried at 70 °C for 2−3 days to obtain a solid mass which was ground into a fine powder. All powders were opaque green except that containing cerium, which appeared dark brown. A custom built hydrothermal autoclave system was used to perform hydrothermal reactions. The system consists of five Inconnel vessels designed to be heated independently and controlled through external temperature controllers. A thermocouple is immersed into the solution within each vessel via an Inconnel insert which enables in situ measurement of the temperature of the solution. Similarly, pressure is measured continually during reactions via electronic read-out. In typical hydrothermal synthesis conditions 300−450 mg of dried amorphous hydroxide powder and 23−25 mL of deionized water was placed inside the Inconnel vessel (filling fraction 50−56% of the total volume capacity of the vessel). No extra base or mineralizer was added, but the hydrothermal synthesis of $LaCrO_3$ was also investigated in presence of the additives KBr, cetyl trimethyl ammonium bromide (CTAB), and sodium dodecyl sulfate (SDS). The initial pH of the suspension containing the amorphous hydroxide powder in deionized water was >10, but after the reaction the pH was observed to be close to neutral. In our reactions the outer heating block was set at 500−600 °C, and in Table 1 the autogenous pressure generated is recorded along with the range of temperatures recorded from within the reaction vessel over the course of the experiment. These conditions lead to the successful formation of well crystalline rare-earth and yttrium orthochromite perovskites in a period of 48 h. Autoclaves were thus heated at 5 °C per minute to reach the desired temperatures and held at that temperature for 24−74 h followed by cooling over 12 h to room temperature. Bright green color precipitates obtained in each reaction were filtered by suction,

(18) Riman, R. E.; Suchanek, W. L.; Lencka, M. M. *Ann. Chim.* **2002**, *27*, 15. Modeshia, D. R.; Walton, R. I. *Chem. Soc Rev.* **2010**, *39*, 4303.
(19) Dutta, P. K.; Gregg, J. R. *Chem. Mater.* **1992**, *4*, 843. Eckert, J. O.; Hung-Houston, C. C.; Gersten, B. L.; Lencka, M. M.; Riman, R. E. *J. Am. Ceram. Soc.* **1996**, *79*, 2929. Fukai, K.; Hidaka, K.; Aoki, M.; Abe, K. *Ceram. Int.* **1990**, *16*, 285. Hertl, W. *J. Am. Ceram. Soc.* **1988**, *71*, 879. Walton, R. I.; Millange, F.; Smith, R. I.; Hansen, T.; O'Hare, D. *J. Am. Chem. Soc.* **2001**, *123*, 12547.
(20) Cheng, H. M.; Ma, J. M.; Zhu, B.; Cui, Y. H. *J. Am. Ceram. Soc.* **1993**, *76*, 625. Cho, S.-B.; Oledzka, M.; Riman, R. E. *J. Cryst. Growth* **2001**, *226*, 313. Gersten, B.; Lencka, M.; Riman, R. *Chem. Mater.* **2002**, *14*, 1950.
(21) Handoko, A. D.; Goh, G. K. L. *Green Chem.* **2010**, *12*, 680.
(22) Wang, D.; Yu, R.; Feng, S.; Zheng, W.; Pang, G.; Zhao, H. *Chem. J. Chin. Univ.* **1998**, *19*, 165. Spooren, J.; Rumplecker, A.; Millange, F.; Walton, R. I. *Chem. Mater.* **2003**, *15*, 1401. Spooren, J.; Walton, R. I. *J. Solid State Chem.* **2005**, *178*, 1683. Spooren, J.; Walton, R. I.; Millange, F. *J. Mater. Chem.* **2005**, *15*, 1542.
(23) Yoshimura, M.; Song, S.; Somiya, S. *Yogyo Kyokai Shi* **1982**, *90*, 9195. Song, S. T.; Pan, H. Y.; Wang, Z.; Yang, B. *Ceram. Int.* **1983**, *10*, 143.
(24) Rivas-Vazquez, L. P.; Rendon-Angeles, J. C.; Rodriguez-Galicia, J. L.; Gutierrez-Chavarria, C. A.; Zhu, K. J.; Yanagisawa, K. *J. Eur. Ceram. Soc.* **2006**, *26*, 81. Rivas-Vazquez, L. P.; Rendon-Angeles, J. C.; Rodriguez-Galicia, J. L.; Zhu, K.; Yanagisawa, K. *Solid State Ionics* **2004**, *172*, 389.
(25) Zheng, W. J.; Pang, W. Q.; Meng, G. Y.; Peng, D. K. *J. Mater. Chem.* **1999**, *9*, 2833.
(26) Ovenstone, J.; Chan, K. C.; Ponton, C. B. *J. Mater. Sci.* **2002**, *37*, 3315.

Table 1. Typical Hydrothermal Reaction Conditions Employed for the Successful Synthesis of Perovskite Orthochromites (48 h Reactions)

compound	solution temperature / °C[a]	autogenous pressure / bar[a]
$YCrO_3$	357−380	190−219
$LaCrO_3$	340−375	171−291
$PrCrO_3$	331−345	170−250
$SmCrO_3$	340−369	220−257
$GdCrO_3$	351−365	238−256
$DyCrO_3$	355−364	228−258
$HoCrO_3$	337−373	171−235
$YbCrO_3$	324−335	230−238

[a] The lowest and highest temperature employed for synthesis of each material corresponds to lowest and highest pressure, respectively recorded inside the solution over the course of a typical hydrothermal reaction.

and washed thoroughly with deionized water several times then dried at 70 °C overnight before further characterization. Twenty-four hours was found to yield rather poorly crystalline powders, and the experimental conditions reported in Table 1 correspond to reactions performed over 48 h.

Characterization. Powder X-ray diffraction (XRD) patterns were collected using a Bruker D8 X-ray diffractometer equipped with CuKα radiation and a VÅNTEC-1 solid-state detector. Lattice parameters were calculated using profile fitting by the Le Bail method (see Supporting Information) employing the computer program GSAS[27] implemented with EXPGUI.[28] XRD patterns from $LaCrO_3$ were also recorded while heating in air in the temperature range of 303−973 K where an Anton-Parr XRK900 heating chamber was used with the sample in static air. The scanning electron microscope (SEM) images of the orthochromite powders were recorded using Zeiss SUPRA 55VP FEG scanning electron microscope. Transmission electron microscopy was performed using a JEOL 2100 LaB_6 instrument, operating at 200 kV. The specimens were dispersed ultrasonically in ethanol and the deposited dropwise onto 3 mm lacey carbon grids supplied by Agar. Raman spectroscopic data on powder samples were recorded at room temperature using Renishaw inVia Raman Microscope equipped with an Ar+ Laser (wavelength 514.5 nm). Magnetization data on all powder samples were measured using a Quantum Design Magnetic Property Measurement System (MPMS) SQUID magnetometer over the temperature region of 2−400 K. Data were collected while cooling (FCC) and then warming (FCW) in a magnetic field. Most of the data were measured with an external applied magnetic field of 100 Oe. For those samples that showed unclear anomalies in 100 Oe, measurements were repeated with higher magnetic field to identify the true nature of the magnetic behavior. Differential scanning calorimetric (DSC) data were collected using a Mettler-Toledo instrument with heating rate of 20 °C min^{-1} in air flow. Thermogravimetric analysis (TGA) and differential thermal analysis (DTA) were performed with a heating rate of 10 °C min^{-1} in air using Mettler-Toledo instruments.

Results and Discussion

When a base is added to a solution containing rare-earth or yttrium(III) chlorides or nitrates and chromium(III) nitrate, a suspension of metal hydroxide is formed in which the mixing of constituent metals is homogeneous, as one would expect in a traditional chemical co-precipitation process. A precipitate from the suspension, when filtered and dried, forms an amorphous powder as evidenced from powder XRD (Supporting Information). Hydrothermal reaction of the amorphous hydroxide precipitates with water within a typical temperature range of 324−380 °C and corresponding pressure range of 170−290 bar produced well crystalline orthochromite perovskites within 24−74 h (Table 1). Given that when a conventional hydrothermal autoclave is heated inside a furnace the temperature of solution inside the autoclave is always likely to be less than the furnace, successful hydrothermal synthesis of well crystalline $LaCrO_3$ powder using reported temperatures up to 700 °C[23] can now be understood. In light of our results, a recent report of a hydrothermal synthesis of $GdCrO_3$ at 150 °C is highly puzzling,[29] although it is not clear in that work whether annealing at higher temperature was actually needed to induce crystallinity.

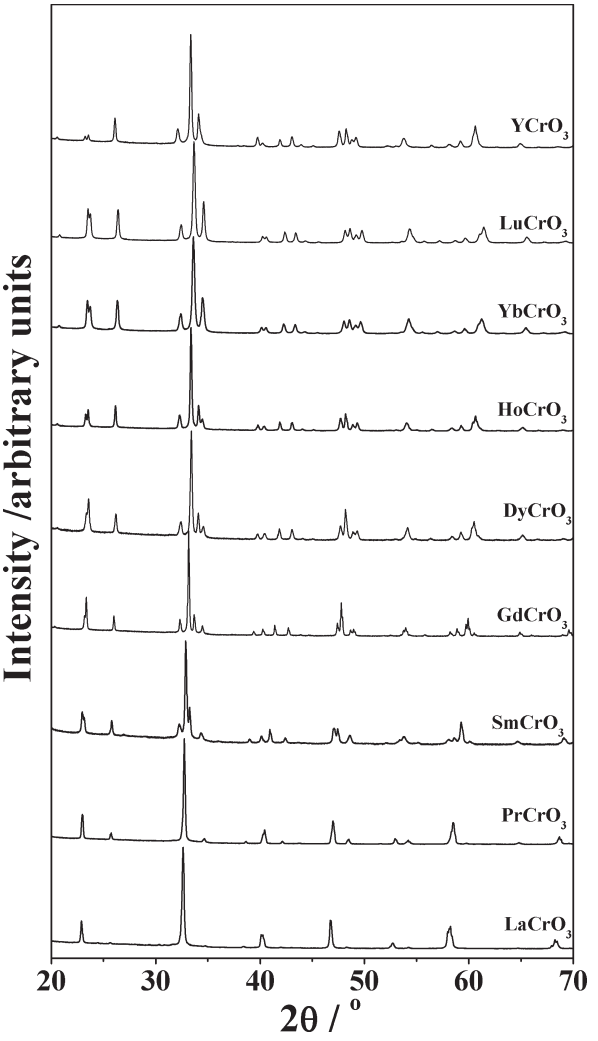

Figure 1. Powder XRD patterns of as-synthesized perovskite rare-earth and yttrium orthochromites (with general formula $RCrO_3$) synthesized under hydrothermal conditions.

Typical powder XRD patterns of as synthesized $RCrO_3$ and $YCrO_3$ powders obtained employing hydrothermal reaction conditions are shown in Figure 1. All the rare-earth

(27) Larson, A. C.; Dreele, R. B. V. Los Alamos National Laboratory Report LAUR 86-748, **1994**.
(28) Toby, B. H. *J. Appl. Crystallogr.* **2001**, *34*, 210.
(29) Jaiswal, A.; Das, R.; Vivekanand, K.; Maity, T.; Abraham, P. M.; Adyanthaya, S.; Poddar, P. *J. Appl. Phys.* **2010**, *107*, 013912.

Table 2. Structural Parameters of Orthorhombic $YCrO_3$ and $RCrO_3$ Perovskites Synthesised under Hydrothermal Conditions[a]

	R_A / Å[b]	a / Å	b / Å	c / Å	V / Å^3	t[c]
$LaCrO_3$	1.216	5.51975(16)	5.49365(10)	7.7766(17)	235.814(10)	0.975
$PrCrO_3$	1.179	5.49572(14)	5.47314(7)	7.71652(8)	232.104(7)	0.954
$SmCrO_3$	1.133	5.36563(8)	5.52357(14)	7.63654(11)	226.328(8)	0.887
$GdCrO_3$	1.107	5.31292(4)	5.52861(6)	7.605444(33)	223.3952(30)	0.875
$DyCrO_3$	1.083	5.26181(7)	5.52554(9)	7.54714(6)	219.428(5)	0.869
$YCrO_3$	1.075	5.25472(12)	5.52043(12)	7.53597(15)	218.606(8)	0.867
$HoCrO_3$	1.072	5.24306(4)	5.53275(5)	7.53411(4)	218.5535(28)	0.866
$YbCrO_3$	1.042	5.20166(7)	5.52496(6)	7.49721(8)	215.462(4)	0.856
$LuCrO_3$	1.032	5.18550(8)	5.52403(7)	7.49406(8)	214.667(5)	0.852

[a] Lattice parameters were obtained by Le Bail profile fitting of respective powder XRD patterns. All orthochromites have space group *Pbnm* (number 62); a, b, c are unit cell constants. [b] R_A is the nine-coordinate ionic radius of respective A site cation.[30] [c] t, the tolerance factor, $= (r_R + r_O)/(\sqrt{2}(r_{Cr} + r_O))$ where r_R, r_O and r_{Cr} are the ionic radii of R^{3+}, O^{2-} and Cr^{3+}, respectively.[30]

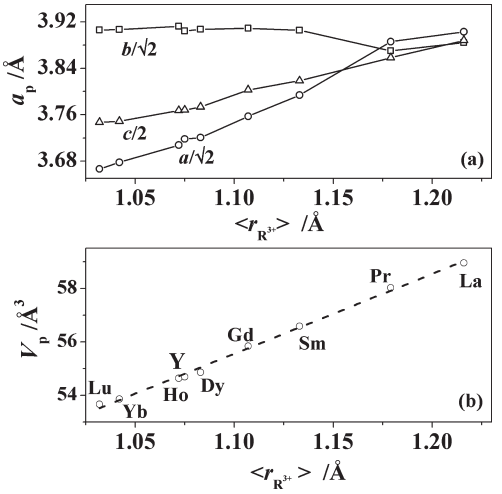

Figure 2. Variation of primitive unit cell (a) lattice parameters (a_P) and (b) volume (V_P) with effective ionic radius (nine-coordination) of rare-earth (and yttrium) orthochromites synthesized under hydrothermal conditions, respectively. The dashed line in (b) is a linear fit to the data (empty circles).

orthochromites and $YCrO_3$ crystallize with an orthorhombic perovskite structure that can be described in standard orthorhombic space group *Pnma* (no. 62) or its non-standard setting *Pbnm*. The unit cell lattice parameters of hydrothermally synthesized perovskite orthochromites were obtained using Le Bail profile fitting, Table 2 (and Supporting Information), using space group *Pbnm*, to allow direct comparison with the materials reported in the literature prepared by conventional synthesis.[2] The lattice parameter values are in excellent agreement with literature values for materials prepared using high temperature, solid-state reactions.[2] In Figures 2a and 2b the variation of the equivalent cubic cell constant, a_p, and primitive unit cell volume (V_p) with effective ionic radius of R^{3+} and Y^{3+} is shown, respectively, using ionic radii taken from tabulated values (note that radii for the A-site metal in nine coordination are used).[30] The unit cell volume of the hydrothermally synthesized perovskite orthochromite family decreases monotonically with effective ionic radius. A linear fit to the unit cell volume data (Figure 2b) indicates that the decrease in unit cell volume in orthochromites is consistent with the expected "lanthanide contraction", which is associated with an increase in structural distortion in the perovskite structure across the rare-earth series from La to Lu.

Hydrothermal reaction of either the suspension containing hydroxides or the amorphous $La_xCr_y(OH)_z$ powder at 240 °C (using conventional Teflon-lined autoclaves) for up to 5 days did not produce any metal oxides; instead a mixture of rare-earth hydroxides $La(OH)_3$ and $LaCO_3OH$ are obtained as the only crystalline products. It is also noteworthy that we are unable to synthesize crystalline $CeCrO_3$ under identical hydrothermal synthesis conditions used for the other $RCrO_3$ materials. Instead, a mixture of crystalline CeO_2 and Cr_2O_3 was always obtained when the amorphous mixed metal hydroxide powder was heated either under hydrothermal reaction conditions or indeed in a furnace (at 600 °C) in air (see Supporting Information). The dark brown color of the dried amorphous hydroxide solid solution powder indicates the change of oxidation state of Ce^{3+} to some Ce^{4+} in the co-precipitated powder itself, although the material is still amorphous. Thus, either a hydrothermal reaction or conventional solid-state heating at the high temperatures fails to produce the perovskite. Conventional approaches to $CeCrO_3$ involve reducing conditions: for example Shukla et al. recently reported a two-step synthesis involving a firing in vacuum in the presence of zirconium sponge as oxygen getter.[31]

Figure 3 shows SEM images of eight of the orthocromites we have prepared. The orthochromites are formed as well-shaped but agglomerated crystallites. The particle size of $LaCrO_3$ (see Figure 4a) and $PrCrO_3$ (Figure 3b) are rather small, and the particles are less agglomerated than in other orthochromites. This is in contrast to the morphology of previously reported hydrothermally synthesized perovskite $LaCrO_3$ synthesized by Zheng et al. who found large microcrystallites when concentrated KOH was used as the reaction medium.[25] The other orthochromites exhibit large agglomerated particles of submicrometer crystallites. A control over particle size and shape is desirable when one wishes to exploit surface-area related properties of perovskite orthochromites.[4] Our preliminary results in this respect are highly promising: Figure 4 shows the morphology of $LaCrO_3$ particles when synthesized either in pure deionized water (at 340 °C and 171 bar, Figure 4a)

(30) Shannon, R. D. *Acta Crystallogr., Sect. A* **1976**, *32*, 751.

(31) Shukla, R.; Bera, A. K.; Yusuf, S. M.; Deshpande, S. K.; Tyagi, A. K.; Hermes, W.; Eul, M.; Pottgen, R. *J. Phys. Chem. C* **2009**, *113*, 12663.

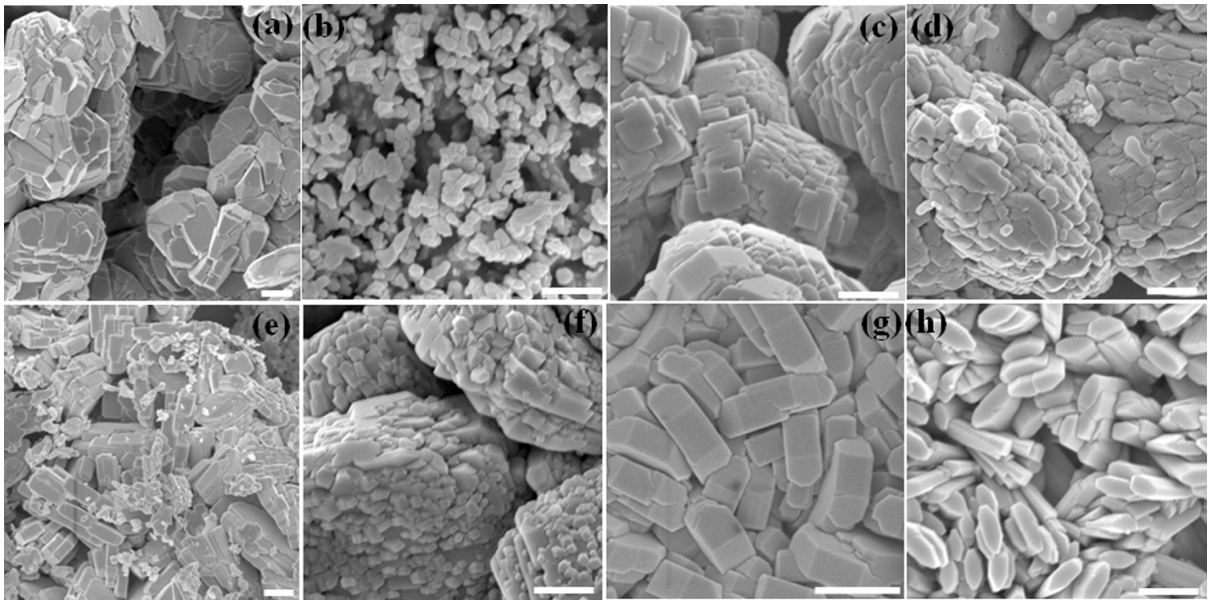

Figure 3. Typical SEM images of perovskite (a) $YCrO_3$, (b) $PrCrO_3$, (c) $SmCrO_3$, (d) $GdCrO_3$, (e) $DyCrO_3$, (f) $HoCrO_3$, (g) $YbCrO_3$, and (h) $LuCrO_3$ powders synthesized under hydrothermal conditions. A scale bar in the right bottom corner of each image is 1 μm.

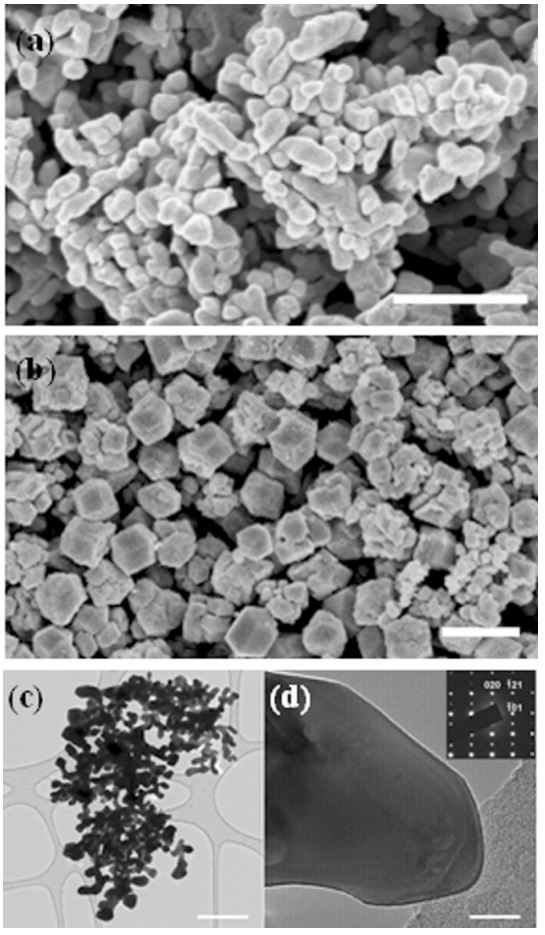

Figure 4. Typical SEM images of hydrothermally synthesized $LaCrO_3$ synthesized in the presence of (a) deionized water, (b) 0.03 M KBr, and (c) and (d) TEM images at two magnifications of the material prepared using 0.005 M SDS. Scale bars are (a) 1 μm, (b) 1 μm, (c) 1 μm, and (d) 20 nm. The inset in (d) shows an indexed SAED, consistent with the powder XRD.

or in the presence of the additives KBr (0.03 M, at 345 °C and 243 bar, Figure 4b), SDS (0.005 M at 361 °C and 241 bar, Figure 4c). In the case of CTAB the product always contained significant amounts of $La(OH)_3$. It is interesting to note that despite the high temperature of the growth solution, the organic additive SDS does influence the morphology of the crystallites, with significantly smaller crystallites formed than in its absence in the same period of time. To investigate the role of inorganic species we included KBr: this results in agglomerates of block shaped crystallites, suggesting that in the case of SDS it is the organic that is influencing the rod-like morphology of the crystallites.

In Figures 5a and 5b we show the temperature dependence of the molar magnetic susceptibility, $\chi_m(T)$, (measured in an applied field of 100 Oe) for all the hydrothermally synthesized perovskite orthochromites. To show clearly any anomalies in the magnetic behavior, we group the data according to the magnitude of the susceptibility below the magnetic ordering temperatures. In all these materials the magnetic moments on the Cr^{3+} ions order antiferromagnetically at T_N, usually with a G-type magnetic structure. This spin-mode leads to weak ferromagnetism below T_N because of a small canting of the Cr moments away from the antiferromagnetic axis. This is most clearly seen in the $\chi_m(T)$ curves for $LuCrO_3$ and $YCrO_3$ where there is no magnetic moment on the rare-earth site (see Figure 5b). These materials order magnetically at $T_N = 115$ and 140 K respectively, and the large signal below T_N is due to the canting of the Cr^{3+} moments. A similar behavior is seen for $LaCrO_3$ ($T_N = 287$ K) but the magnitude of χ_m below T_N is reduced, suggesting that the canting angle is much smaller (inset (iii) in Figure 5b). We attribute the upturn seen in the magnetization of $LaCrO_3$ at low temperature (20 to 2 K) to a small quantity of (para)magnetic impurities which are commonly present in commercial rare-earth compounds (the starting material in synthesis). The upturn is visible in these data only because the overall magnitude of the susceptibility is very small ($\sim 9 \times 10^{-3}$ emu/mol at 20 K).

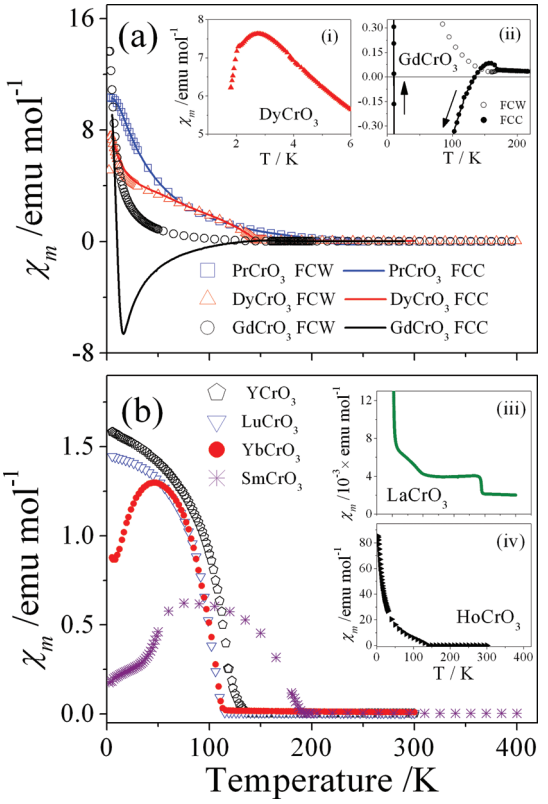

Figure 5. Temperature dependence of the magnetic susceptibility per mol (χ_m) of hydrothermally synthesized perovskite orthochromites, measured in an applied field of 100 Oe. (a) Field-cooled warming, FCW, (symbols) and field-cooled cooling, FCC, (lines) curves of $PrCrO_3$, $DyCrO_3$, and $GdCrO_3$. Insets in (a) show (i) the onset of a magnetic ordering of the Dy^{3+} moments in $DyCrO_3$ at 2.3 K and (ii) a negative magnetization during FC cooling in $GdCrO_3$ because of a polarization of the Gd^{3+} moments antiparallel to the ferromagnetic component of the canted Cr^{3+} spins. (b) FCW curves for $YCrO_3$, $LuCrO_3$, $YbCrO_3$, $SmCrO_3$, $LaCrO_3$ (inset (iii)), and $HoCrO_3$ (inset (iv)).

For all the other materials prepared, the R^{3+} rare-earth ions also carry a magnetic moment which can couple with the Cr^{3+} spin structure. The orientation of the rare-earth moments with respect the Cr^{3+} spins depends on the nature of the effective magnetic field at the rare-earth site. This is clearly seen in the data for $PrCrO_3$, $DyCrO_3$, and $HoCrO_3$ in which the Cr^{3+} spins order magnetically at T_N = 238, 145, and 142 K, respectively. We note that for these materials there is no difference between the field-cooled warming (FCW) and field-cooled cooling (FCC) magnetization curves suggesting that for these materials the moments on the R^{3+} sites lie parallel to the ferromagnetic component of the ordered Cr^{3+} spins. At low temperature the R^{3+} moments may also order. For example, the maximum in the $\chi_m(T)$ curve of $DyCrO_3$ (see inset (i) in Figure 5a) at 3.5 K is associated with an onset of antiferromagnetic ordering of Dy^{3+} spins with a T_{N2} of 2.2 K.[32] For $PrCrO_3$ and $HoCrO_3$ the susceptibility flattens at low-temperature, but there are no features in the $\chi_m(T)$ curves above 1.7 K that can clearly be associated with an ordering of the R^{3+} moments.

The consequences of the coupling between the R^{3+} and the Cr^{3+} spins is perhaps most dramatically demonstrated in $GdCrO_3$. There is a considerable difference between the FCW and FCC data for this material below T_N = 169 K. On cooling, the magnetization increases abruptly at T_N, but then becomes negative below 135 K before passing through zero again at 10 K (see inset (ii) in Figure 5a). On heating, the magnetization decreases but remains positive up to T_N. It has been suggested that the anomalous behavior in the magnetization of $GdCrO_3$ is due to a polarization of the paramagnetic Gd^{3+} moments antiparallel to the ferromagnetic component arising from the canted antiferromagnetically ordered Cr^{3+} moments.[33] A maximum in $\chi_m(T)$ suggests that the Gd^{3+} moments eventually order at ~2.3 K. In $YbCrO_3$, the Cr^{3+} spins are ordered below T_N = 115 K. Here again, the net reduction in $\chi_m(T)$ below 40 K (Figure 5b) is attributed to an antiparallel coupling between the moments on the Yb^{3+} ions and the weak ferromagnetic component of the Cr^{3+} spins.[33] Upon further cooling, the magnetization increases between 7 and 3 K, corresponding to the onset of antiferromagnetic ordering of Yb^{3+} spins (T_N = 3.05 K).[1] In $SmCrO_3$ (T_N = 192 K) the coupling between the Sm^{3+} and Cr^{3+} spins is responsible for a spin reorientation at ~33 K. The ordering temperatures for the hydrothermally prepared $RCrO_3$ materials, along with previously reported values determined using neutron diffraction or magnetization measurements on either polycrystalline or single-crystal materials, are given in Table 3. The values of T_N for the present samples are in good agreement with the reported values from samples prepared using conventional synthesis, varying from 295 K for $LaCrO_3$ to 111 K for $LuCrO_3$.

Figure 6, shows the reciprocal of molar magnetic susceptibility as a function of temperature for all the of hydrothermally synthesized perovskite orthochromites. The materials all exhibit Curie−Weiss behavior above T_N and the data can be fitted using $\chi_m(T) = C/(T - \theta) + \chi_0$ where C is the Curie constant, θ is the Weiss temperature, and χ_0 is a temperature independent contribution to the magnetic susceptibility arising from sources such as the electron cores. For the samples where there is a reasonable temperature interval (>100 K) between T_N and 400 K, the maximum temperature used for the measurements, there is good agreement between the θ and C values determined from our data and the experimental values reported in the literature. C can be used to evaluate the effective moment on the R^{3+} and the Cr^{3+} ions. For the materials containing Y^{3+} or the rare-earth ions Pr^{3+}, Dy^{3+}, Ho^{3+}, Gd^{3+}, and Yb^{3+}, the calculated effective moments are consistent with a full-J effective moment on the rare earth sites along with a spin-only moment of 3.87 μ_B/Cr^{3+}. This further confirms that the oxidation state of the chromium in hydrothermally synthesized perovskite orthochromites remains as 3+.

Analysis of the data for $LaCrO_3$ (and to a lesser extent the Sm and Lu compounds) is made difficult by the high T_N, the low moment, and the narrow experimental temperature

(32) Laar, B. V.; Elemans, B. A. A. *J. Phys.* (*Paris*) **1971**, *32*, 301.

(33) Kojima, N.; Tsushima, K.; Kurita, S.; Tsujikawa, I. *J. Phys. Soc. Jpn.* **1980**, *49*, 1456.

Table 3. Magnetic Parameters Derived from the Magnetization Measurements of the Perovskite Orthochromite Powders Synthesized under Hydrothermal Conditions[a]

	T_N / K[b]		$\|\theta\|$ / K		C		μ_{eff}	$\mu_{R^{3+}}$		$\mu_{Cr^{3+}}$	
$RCrO_3$	this work	published data	this work	published data	this work	published data	this work	this work[c]	$g[J(J+1)]^{1/2}$	this work[d]	$2[S(S+1)]^{1/2}S = 3/2$
$YCrO_3$	140	141[1,5,6]	260	230,[5] 315,[1] 360[6]	1.84	1.20,[34] 2.13[1]	3.84	0	0	3.84	3.87
$LaCrO_3$	287	282,[1] 295,[35] 288[36]	750	800[1]	3.3	2.41[1]	5.14	0	0	5.14	3.87
$PrCrO_3$	238	237,[37] 239,[1] 240[36]	188	205[1]	3.39	2.35[1]	5.21	3.52	3.58	3.78	3.87
$SmCrO_3$	192	192,[5] 190,[38] 193[1]	670	[e]	3.73	2.26[1]	5.46	4.43	0.84	5.39	3.87
$GdCrO_3$	169	170[1]	25	35,[39] 58[1]	8.39	9.65[1]	8.2	7.22	7.94	2.02	3.87
$DyCrO_3$	145	146[5,6]	37	12[34]	15.5	19.1[34]	11.13	10.45	10.63	3.3	3.87
$HoCrO_3$	142	141[5]	19	12[34]	14.9	19.1[34]	10.93	10.23	10.6	2.67	3.87
$YbCrO_3$	115	118[5]	102	140[34]	4.27	4.4[34]	5.84	4.4	4.54	3.67	3.87
$LuCrO_3$	115	112,[5] 111,[40] 115[6]	129	274[6]	2.54	[e]	4.51	0	0	4.51	3.87

[a] The table also contains the corresponding values taken from previously published work. [b] T_N is the antiferromagnetic Neel temperature associated with the ordering of unpaired spins of Cr^{3+}. θ, the Weiss temperature, and C, the Curie constant, are evaluated from the Curie-Weiss law: The molar magnetic susceptibility $\chi_m(T) = C/(T-\theta)+\chi_0$. The effective magnetic moment $\mu_{eff} = [(\mu_{R^{3+}})^2 + (\mu_{Cr^{3+}})^2]^{1/2} = [3k_BC/N_A\mu_B]^{1/2}$ where N_A is Avogadro's number, k_B is the Boltzmann constant and the μ_B is the Bohr magneton. [c] $\mu_{R^{3+}}$ is calculated assuming $S = {}^3/_2$ on the Cr site. [d] $\mu_{Cr^{3+}}$ is calculated assuming a full J moment on the R^{3+} site. [e] Either unavailable in the literature, or not calculated (see text).

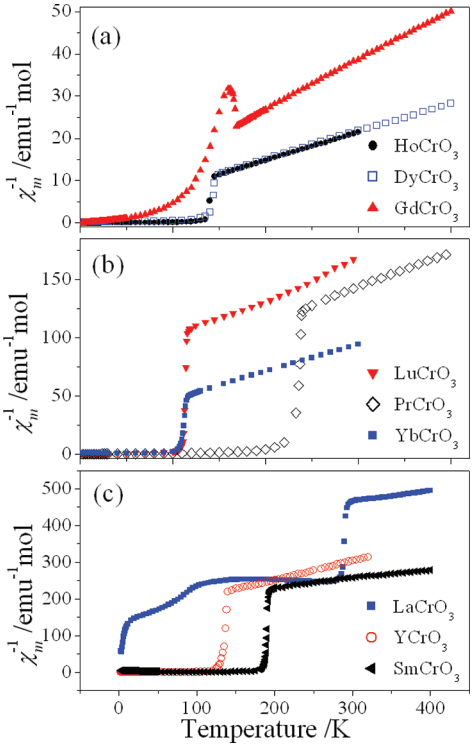

Figure 6. Variation of inverse molar magnetic susceptibilities χ_m^{-1} with temperature for the perovskite rare-earth and yttrium orthochromites synthesized under hydrothermal conditions. All the data were collected during heating with an applied magnetic field of 100 Oe.

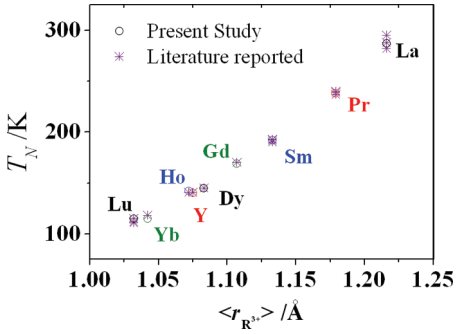

Figure 7. Antiferromagnetic Néel temperature (T_N), characterizing the ordering of the unpaired Cr^{3+} spins in the perovskite orthochromites synthesized under hydrothermal conditions, as a function of the average ionic radii of the A site ion ($\langle r_R \rangle$ nine co-ordination) in the perovskite structure. T_N values were determined using $\chi_m(T)$ data. Literature values were taken from the references in Table 3.

window in which the sample is expected to be paramagnetic. Fixing χ_0 at $\sim 2 \times 10^{-3}$ emu/mol and fitting between 330 and 400 K gives a reasonable value for the moment on Cr^{3+}. A fitted value for θ of 750 K, however, appears high for a paramagnetic sample with a T_N of 287 K. To the best of our knowledge, the only other reported value for θ in $LaCrO_3$ is 800 K[1] and this also appears high. We note, however, that the value for $YCrO_3$ is also almost double the ordering temperature, perhaps indicating that a degree of frustration is present within these systems. Studies to higher temperatures would be required to obtain more reliable information on the behavior of $LaCrO_3$ in the paramagnetic state.

Figure 7 shows how T_N for the $RCrO_3$ materials increases with ionic radius of the A site cation radius (rare-earth and yttrium ions) in the orthochromite series. Similar correlations have been observed for the rare-earth manganites $RMnO_3$ where the Mn−O−Mn bond angle reduces as the radius of the rare-earth cation is decreased, thus affecting magnetic interaction of the B-site metals.[41] We do note that the situation with the manganites is more complex since the octahedral Mn^{3+} ion is Jahn−Teller distorted and there are also magnetic phase transitions seen in manganites with A-site radius.

The orthorhombic perovskites (space group *Pnma*) are expected to have 24 Raman-active phonon modes

(34) Lal, H. B.; Gaur, K.; Dwivedi, R. D. *J. Mater. Sci. Lett.* **1995**, *14*, 9.
(35) Weinburg, I.; Larsen, P. *Nature* **1961**, 192.
(36) Yoshii, K. *J. Alloys Compd.* **2000**, *305*, 72.
(37) Gordon, J. D.; Hornreich, R. M.; Shtrikman, S.; Wanklyn, B. M. *Phys. Rev. B* **1976**, *13*, 3012.
(38) Gorodetsky, G.; Hornreich, R. M.; Shaft, S.; Sharon, B.; Shaulov, A.; Wanklyn, B. M. *Phys. Rev. B* **1977**, *16*, 515.
(39) Yoshii, K. *J. Solid State Chem.* **2001**, *159*, 204.
(40) Hornreich, R. M.; Shtrikman, S.; Wanklyn, B. M.; Yaeger, I. *Phys. Rev. B* **1976**, *13*, 4046.
(41) Kimura, T.; Ishihara, S.; Shintani, H.; Arima, T.; Takahashi, K. T.; Ishizaka, K.; Tokura, Y. *Phys. Rev. B* **2003**, 68.

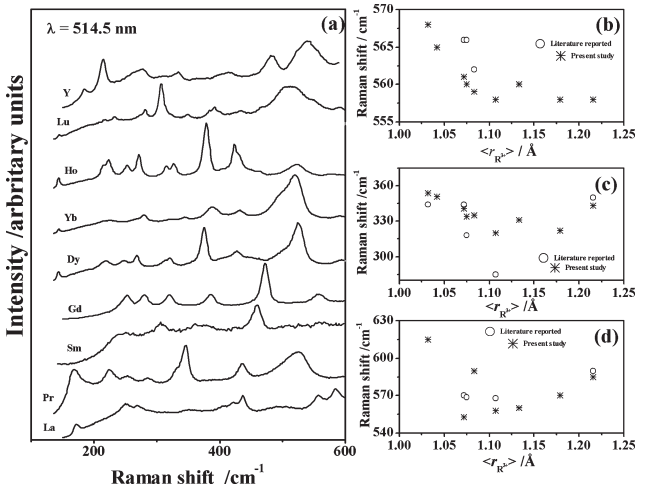

Figure 8. (a) Raman spectra of hydrothermally synthesized polycrystalline $RCrO_3$ perovskite yttrium and rare-earth orthochromites (denoted with the R element symbol). Dependence of selected (b) A_{1g} (~560 cm^{-1}), (c) B_{2g} (~330 cm^{-1}), and (d) B_{3g} (~540 cm^{-1}) phonon modes (see Supporting Information available) with average ionic radii (nine coordination) of yttrium and rare-earth ions. Literature reported values were taken from references.[29,44].

($7A_{1g}$, $5B_{1g}$, $7B_{2g}$ and $5B_{3g}$).[42,43] The origin of corresponding Raman bands in the observed spectra are mainly due to four different types of distortion in the structure. Rotation of BO_6 octahedra along [010] and [101] axes, Jahn−Teller distortion, and shift of A atom from its position in the ideal cubic perovskite structure.[43] However, the experimentally observed number of modes is less. The Raman spectra of a few orthochromites $RCrO_3$ (where R = Y, La, Gd and Ho) have been reported in the literature whereas spectra of R = Sm, Dy, Yb, Lu are not known.[29,42,44] Figure 8a shows the Raman spectra recorded at room temperature from polycrystalline powders of hydrothermally synthesized $YCrO_3$ and $RCrO_3$. Although not all samples showed presence of all the Raman active modes predicted from group theory analysis, we can see at least two important Raman modes (namely one A_{1g} mode ~560 cm^{-1} and one B_{2g} mode ~320 cm^{-1}) present in Raman spectra of all the perovskite orthochromites. The quality of spectra is much better than previously reported spectra of polycrystalline $GdCrO_3$,[29] owing to the high crystallinity of our hydrothermally derived samples. Because of the discrepancies over assignment of phonon modes of $RCrO_3$ in single-crystalline materials in the literature,[44] as well as absence of some bands in the spectra of polycrystalline samples, we are unable to assign unequivocably all observed Raman bands. However, we have tentatively assigned the bands and compare the Raman band positions of $YCrO_3$, $LaCrO_3$, $GdCrO_3$, and $HoCrO_3$ with the literature reported values (see Supporting Information).

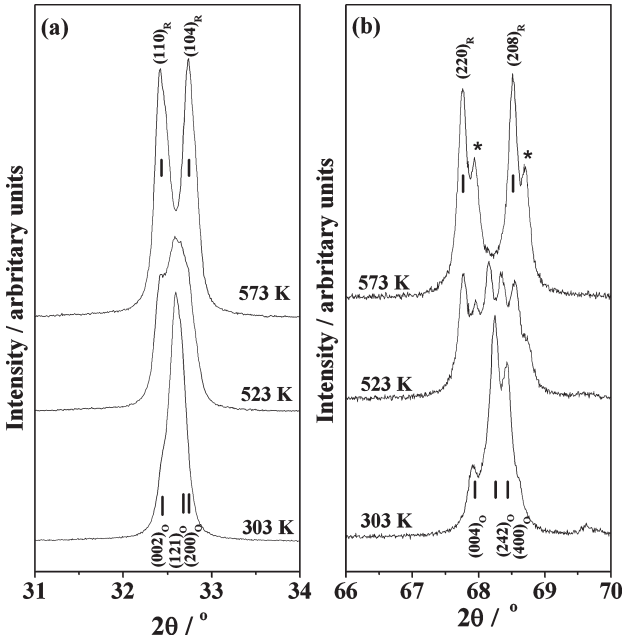

Figure 9. Portions of XRD patterns of $LaCrO_3$ powder at 303, 523, and 573 K. Tick marks indicate peak positions, suffixes R and O corresponds to Miller indices of peaks of rhombohedral ($R\bar{3}c$) and orthorhombic (*Pnma*) phases, respectively. * denote peaks due to Cu Kα2.

In Figure 8b we plot frequency of specific A_{1g} and B_{2g} modes as a function of rare earth ionic radius. It is apparent that the selected A_{1g} (at around 560 cm^{-1}, Figure 8b) and B_{2g} (at around 325 cm^{-1}, Figure 8c) modes soften with increasing rare-earth size, indicating reduction of distortion of CrO_6 octahedra as we move from Lu to La in the rare earth orthochromite series, as expected.

$LaCrO_3$ is known to undergo a first-order structural phase transition between orthorhombic and rhombohedral (between space group *Pnma* with $a^-a^-b^+$ tilt system to space group $R\bar{3}c$, with $a^-a^-a^-$ tilt system[45]) phases in the temperature range of 528−550 K.[46,47] Figure 9 shows enlarged view of two selected regions of XRD pattern of the hydrothermally prepared $LaCrO_3$ at, 303, 523, and 573 K (XRD patterns within the temperature range of 303−973 K are given in the Supporting Information). The thermal evolution of rhombohedral symmetry in hydrothermally synthesized $LaCrO_3$ is clearly observed by the appearance of (110) (2θ = 32.419°), (104) (2θ = 32.736°), (220) (2θ = 67.759°), and (208) (2θ = 68.519°) in the powder XRD pattern recorded at 573 K (Figure 9a). Thus, the XRD pattern at 523 K is that of a mixture of orthorhombic and rhombohedral phases, and $LaCrO_3$ exists as pure rhombohedral phase at 573 K. The lattice parameters obtained from the Rietveld refinement of laboratory XRD data at 573 K for rhombohedral $LaCrO_3$ are a = 5.52972(5) Å and c = 13.35391(14) Å

(42) Iliev, M. N.; Abrashev, M. V.; Lee, H. G.; Popov, V. N.; Sun, Y. Y.; Thomsen, C.; Meng, R. L.; Chu, C. W. *Phys. Rev. B* **1998**, *57*, 2872.
(43) Abrashev, M. V.; Bäckström, J.; Börjesson, L.; Popov, V. N.; Chakalov, R. A.; Kolev, N.; Meng, R. L.; Iliev, M. N. *Phys. Rev. B* **2002**, 65.
(44) Iliev, M. N.; Litvinchuk, A. P.; Hadjiev, V. G.; Wang, Y. Q.; Cmaidalka, J.; Meng, R. L.; Sun, Y. Y.; Kolev, N.; Abrashev, M. V. *Phys. Rev. B* **2006**, 74. Kaczmarek, W.; Morke, I. *J. Magn. Magn. Mater*. **1986**, *58*, 91. Udagawa, M.; Kohn, K.; Koshizuka, N.; Tsushima, T.; Tsushima, K. *Solid State Commun*. **1975**, *16*, 779.
(45) Glazer, A. M. *Acta Crystallogr., Sect. B* **1972**, *28*, 3384.
(46) Geller, S.; Raccah, P. M. *Phys. Rev. B* **1970**, *2*, 1167. Hashimoto, T.; Tsuzuki, N.; Kishi, A.; Takagi, K.; Tsuda, K.; Tanaka, M.; Oikawa, K.; Kamiyama, T.; Yoshida, K.; Tagawa, H.; Dokiya, M. *Solid State Ionics* **2000**, *132*, 181. Hofer, H. E.; Kock, W. F. *J. Electrochem. Soc*. **1993**, *140*, 2889. Momin, A. C.; Mirza, E. B.; Mathews, M. D. *J. Mater. Sci. Lett*. **1991**, *10*, 1246.
(47) Oikawa, K.; Kamiyama, T.; Hashimoto, T.; Shimojyo, Y.; Morii, Y. *J. Solid State Chem*. **2000**, *154*, 524.

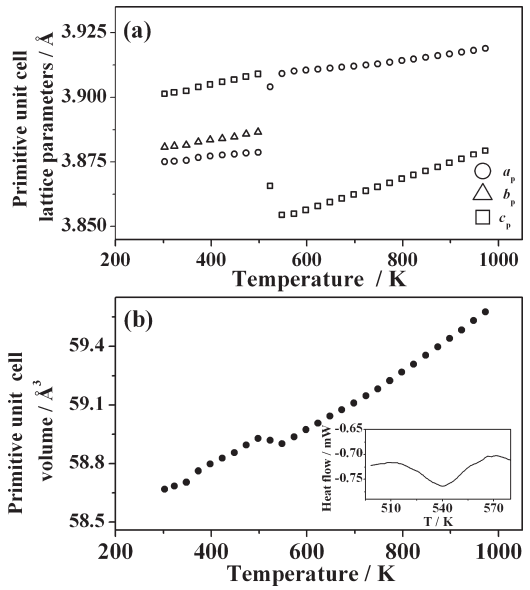

Figure 10. Variation of primitive unit cell lattice parameters (a_p, b_p, and c_p) and volume (V_p), respectively, with temperature when hydrothermally synthesized polycrystalline $LaCrO_3$ powder is heated. Change of the (a) a_p, b_p, and c_p calculated from respective unit cell parameters of *Pnma* and $R\bar{3}c$ phases and (b) V_p, respectively as a function of temperature. Inset in (b) is DSC curve of hydrothermally synthesized $LaCrO_3$ powder showing an endothermic peak due to the structural phase transition.

and agree well with the reported values at 593 K (a = 5.53049 (11) Å, c = 13.3544(3) Å).[47] The primitive cell (pseudocubic) lattice parameters, a_p, b_p, and c_p have been evaluated from the Rietveld refinement of powder XRD patterns at each temperature in the temperature range of 303−973 K. The a_p, b_p, and c_p are related to the unit cell parameters of orthorhombic and rhombohedral phases by the following relationships: orthorhombic (*Pnma* setting) lattice parameters are $a_O = a_p\sqrt{2}$, $b_O = 2a_p$, $c_O = a_p\sqrt{2}$ and rhombohedral ($R\bar{3}c$) lattice parameters are $a_R = a_p\sqrt{2}$ and $c_R = a_p 2\sqrt{3}$. Variation of a_p, b_p, and c_p with temperature are shown in Figure 10a. Also the variation of primitive unit cell volume (V_p) with temperature is shown in Figure 10b. The orthorhombic-rhombohedral phase transition is associated with an increase of a_p and decrease of c_p. Thus, the V_p changes its slope while passing through the transition temperature. The coefficients of volume thermal expansion are calculated to be 2.273×10^{-5} K^{-1} for orthorhombic and 2.713×10^{-5} K^{-1} for rhombohedral phases. The volume thermal expansion coefficient values are in the same order of magnitude with the literature reported values (2.285(16) $\times$ 10^{-5} K^{-1} and 2.842(12) $\times$ 10^{-5} K^{-1} for orthorhombic and rhombohedral phases, respectively[47]). An endothermic peak in the DSC curve (see inset in Figure 10b) gave a temperature of 540 K for the phase transition in hydrothermally synthesized $LaCrO_3$ polycrystalline powder, in good agreement with the powder XRD (548 K) and the previous literature for samples prepared by solid-state synthesis.

Conclusions

We have systematically explored a soft-chemical, hydrothermal route for the synthesis of polycrystalline rare-earth and yttrium orthochromite perovskites. The general procedure adopted is applicable across the lanthanide series, except in the case of $CeCrO_3$, which may be ascribed to the ease of formation of Ce^{4+} under the oxidizing conditions of water heated in excess of 300 °C. Unlike previous reports of hydrothermal synthesis of other perovskite oxides, such as titanates, niobates, and manganites, the synthesis of the orthochromites requires significantly higher temperatures (> 300 °C), and this may be due in part to the kinetic stability of octahedral Cr(III) in solution. The investigation of magnetic properties of hydrothermally synthesized orthochromite perovskites reveals the high quality of the polycrystalline samples, and comparison with the available literature data on materials prepared by high temperature annealing would suggest that the hydrothermal samples are free of any significant quantities of hydroxide or water, since their magnetic characteristics resemble single crystalline specimens. Finally we have presented some preliminary evidence of control over particle size and shape in the presence of solution additives in synthesis, even when under these relatively severe reaction conditions; this could be of importance in future applications of the materials.

Acknowledgment. We thank the EPSRC for funding this work (EP/F012721), and Mr. David Gorman of Baskerville Ltd for help with the design of the multicell hydrothermal reactor. Some of the equipment used in materials characterization at the University of Warwick was obtained through the Science City Advanced Materials project "Creating and Characterising Next Generation Advanced Materials" with support from Advantage West Midlands (AWM) and part funded by the European Regional Development Fund (ERDF).

Supporting Information Available: Further details are given in Figures S1−S5 and Table S1. This material is available free of charge via the Internet at http://pubs.acs.org.